


Article

Deflection Angle of Photons through Dark Matter by Black Holes and Wormholes Using Gauss–Bonnet Theorem

Ali Övgün ^{1,2} 

¹ Instituto de Física, Pontificia Universidad Católica de Valparaíso, Casilla 4950, Valparaíso, Chile; ali.ovgun@pucv.cl

² Physics Department, Arts and Sciences Faculty, Eastern Mediterranean University, North Cyprus via Mersin 10, Famagusta 99628, Turkey; ali.ovgun@emu.edu.tr

Received: 17 March 2019; Accepted: 9 May 2019; Published: 14 May 2019



Abstract: In this research, we used the Gibbons–Werner method (Gauss–Bonnet theorem) on the optical geometry of a black hole and wormhole, extending the calculation of weak gravitational lensing within the Maxwell’s fish eye-like profile and dark-matter medium. The angle is seen as a partially topological effect, and the Gibbons–Werner method can be used on any asymptotically flat Riemannian optical geometry of compact objects in a dark-matter medium.

Keywords: gravitational lensing; weak deflection; dark matter; Gauss–Bonnet theorem; black hole; wormhole

PACS: 95.30.Sf; 98.62.Sb; 97.60.Lf

1. Introduction

Black holes are an essential component of our universe, and one of the most important discoveries in astrophysics is that, when stars die, they can collapse to become extremely small objects. Black holes provide an important opportunity for probing and testing the fundamental laws of the universe. For example, gravitational waves from black holes and neutron star mergers have been recently detected [1]. Black holes may also hint at the nature of quantum gravity at small scales that change the area law of entropy. Quantum gravity is far from understood, though theoretically it has seen tremendous progress, and, in a few years, the Event Horizon Telescope may provide some more information about it [2–5].

In 1854, Maxwell presented the solution to a mathematical problem related to the passage of rays through a sphere of variable refractive index, and he noted that the potential existence of a medium of this kind would possess exceptional optical properties [6]. This is similar to the reflection of the crystalline lens in fish. This optical tool is Maxwell’s fish eye (MFE), the condition in which all light rays form circular trajectories. It was a remarkable accomplishment to visualize that a lens whose refractive index increases toward a point could form perfect images [7].

Luneburg discovered that the ray propagation of MFE is equivalent to ray propagation on a homogeneous sphere with a unit radius and a unit refractive index within geometrical optics [8]. This showed that the imaging of variants that have been applied to microwave devices and the fish-eye lens in photography form an extremely wide-angled image, almost hemispherical in coverage. In 2009, Leonhardt showed that MFE is also good for waves, and it enables the production of super-resolution imaging with perfect lensing, which requires negative refractive-index materials. This began a debate and offered a rich area of research to explore [9–11]. It was shown that perfect imaging in a homogeneous three-dimensional region is also possible [12]. MFE happens when all light rays

arising from any point within converge at its conjugate, which means that power released from a source can only be fully absorbed at its image point, resulting in perfect imaging. There has been a rapid increase in the importance of perfect imaging in theoretical and experimental optics [13–15].

Fermat’s principle says that light rays always follow extremal optical paths, with path length being measured by refractive index n . The formula for MFE indicates the interesting possibility that rays generate a perfect image in a black hole. The refractive index depends only on distance r from the origin [13,14]. In this paper, we try to understand the effect of an MFE-like profile on the deflection angle. For simplicity, we used the uniform MFE-like profile, which is different from a nonuniform MFE profile.

Gravitational lensing is a useful tool of astronomy and astrophysics [16], in which light rays from distant stars and galaxies are deflected by a planet, a black hole, or dark matter [17,18]. The detection of dark-matter filaments [19] using weak deflection is a very relevant topic because it can help in understanding the large-scale structure of the universe [20]. To build a sky map (the refractive index of the entire visible universe), there is ongoing research on the observation of the effect of cosmological weak deflection on temperature fluctuations in the cosmic microwave background (CMB) [21]. From a theoretical point of view, new methods have been proposed to calculate deflection angle. One of them is the Gauss–Bonnet theorem (GBT), which was first proposed by Gibbons and Werner using optical geometry [22–24]. The deflection angle is seen as a partially topological effect that can be calculated by integrating the Gaussian curvature of the optical metric outward from the light ray by using the following equation: [22,23]

$$\hat{\alpha} = - \int \int_{D_\infty} K dA. \quad (1)$$

Since Gibbons and Werner’s paper on weak deflection angles by GBT provided a unique perspective, this method has been applied in various cases [25–47].

Dark matter makes up to 27% of the total mass–energy of the universe [48]. We can only detect dark matter from its gravitational interactions, and we only know that dark matter is nonbaryonic, nonrelativistic (or cold), and it has weak nongravitational interactions. There are many dark-matter candidates, such as weakly interacting massive particles (WIMPs), super-WIMPs, axions, and sterile neutrinos [49]. It has been proposed that dark matter is a composite, such as the dark-atom model, which we investigate here using the deflection of light through it. Dark matter, although suppressed, generally has electromagnetic interactions [50], such that the medium of dark matter should have some optical properties that a traveling photon can sense because of the frequency-dependent refractive index. The refractive index regulates the speed at which a wave is propagated via a medium. The particles of dark matter do not get electrically charged, but they can couple to other particles that have a virtual electromagnetic charge, and can also couple to photons [51–54]. To find the amplitude of dark-matter annihilation into two photons, we must first calculate the scattering amplitude. One can obtain the index of the refractive of light, where the real part is related to the speed of propagation.

To investigate weak deflection through dark matter, we consider the propagation effects for the case that particles of dark matter (warm thermal relics or axionlike particles) have low mass whose number density is larger than ordinary matter. Put simply, dark matter interacts with photons (if only through quantum fluctuations), resulting in a refractive index. The relationship between refractive index and the forward Compton amplitude at relatively low photon energies [50] ($\mathcal{M}_{\text{fwd}} \sim -\epsilon^2 e^2$) is

$$n = 1 + \frac{\rho}{4m_{dm}^2 \omega^2} \mathcal{M}_{\text{fwd}}, \quad (2)$$

where ω is the measured photon frequency, and $\rho = 1.1 \times 10^{-6} \text{ GeV/cm}^3$ is the present-day dark-matter density [50]. Neglecting spin, the amplitude is a real and even function of ω (for photon energies below the inelastic threshold); additionally, the coefficients of the $O(\omega^{2n})$ terms are positive

and spin-dependent interactions can lead to odd powers in the expansion about ω . Their presence could give information on the spin of dark matter. Hence, the refractive index becomes [50]:

$$n = 1 + \frac{\rho}{4m_{dm}^2} \left[\frac{A}{\omega^2} + B + C\omega^2 + \mathcal{O}(\omega^4) \right]. \quad (3)$$

To do so, we suppose that photons can be deflected through dark matter due to dispersive effects. We used the index of refractive $n(\omega)$ that is manipulated by the scattering amplitude of the light and dark matter in the forward [50].

Gravitational lensing in plasma has been studied in various cases [45,46,55–57]. For the first time, Bisnovatyi-Kogan and Latimer showed that, due to the dispersive properties of plasma, even in homogeneous plasma, gravitational deflection differs from a vacuum deflection angle [56,57]. Moreover, it was shown that the deflection angle is increased due to the presence of plasma [55]. Afterward, Crisnejo and Gallo calculated weak lensing in a plasma medium using the GBT [45].

The main motivation of this research is to shed light on the unexpected features of spacetimes in regards to an MFE-like profile, and to derive the deflection angle of black holes using the Gauss–Bonnet theorem in weak limits for a dark-matter medium. We suppose that the refractive index of the medium is spatially nonuniform but it is uniform at large distances. We also investigated the effect of various parameters on the refractive index of the medium, which has not been covered in previous studies.

2. Effect of Medium on Deflection Angle of Schwarzschild Black Hole Using Gauss–Bonnet Theorem

In this section, we first describe the black-hole solution in a static and spherically symmetric spacetime. Then, we apply the MFE-like profile within the GBT to calculate the weak deflection angle.

The Schwarzschild black-hole spacetime reads

$$ds^2 = -f(r)dt^2 + g(r)dr^2 + r^2(d\theta^2 + \sin^2\theta d\varphi^2), \quad (4)$$

with metric functions

$$f(r) = g(r)^{-1} = 1 - \frac{2M}{r}. \quad (5)$$

Analysis of the geodesics equation, the ray equation, is calculated by

$$\varphi = \int \frac{b\sqrt{g(r)}dr}{r^2\sqrt{\frac{1}{f(r)} - \frac{b^2}{r^2}}}, \quad (6)$$

where b is the impact parameter of the unperturbed photon.

Our universe is homogeneous and isotropic on large scales. Now, we consider isotropic coordinates that are nonsingular at the horizon and time direction is a Killing vector. Moreover, time slices become Euclidean with a conformal factor, and one can calculate refractive index n of light rays around the black hole. Another important feature of isotropic coordinates is that they satisfy Landau's condition of coordinate clock synchronization:

$$\frac{\partial}{\partial x_j} \left(-\frac{g_{0i}}{g_{00}} \right) = \frac{\partial}{\partial x_i} \left(-\frac{g_{0j}}{g_{00}} \right) (i, j = 1, 2, 3). \quad (7)$$

Using transformation

$$r = \rho \left(1 + \frac{M}{2\rho} \right)^2, \quad (8)$$

the Schwarzschild black hole is rewritten in isotropic coordinates (where ρ is an isotropic radial coordinate) [45]

$$ds^2 = -F(\rho)dt^2 + G(\rho)(d\rho^2 + \rho^2 d\Omega^2), \quad (9)$$

with

$$F(\rho) = \left(\frac{\rho - \frac{M}{2}}{\rho + \frac{M}{2}} \right)^2, \text{ and } G(\rho) = \left(\frac{\rho + \frac{M}{2}}{\rho} \right)^4. \quad (10)$$

The metric becomes nonsingular at horizon $r = 2M$. It can also be written in Fermat form of the metric:

$$ds^2 = F(\rho)[-dt^2 + n(\rho)^2(d\rho^2 + \rho^2 d\Omega^2)], \quad (11)$$

with index of refractive $n(\rho) = \frac{c}{v(\rho)}$. For the Schwarzschild black-hole medium, the refractive index reads

$$n = \frac{\left(1 + \frac{M}{2\rho}\right)^3}{\left(1 - \frac{M}{2\rho}\right)}, \quad (12)$$

and it can be approximated for large $\rho \gg M$

$$n \approx 1 + \frac{2M}{\rho}. \quad (13)$$

Now, the ray equation becomes

$$\varphi = \int \frac{b d\rho}{\rho^2 \sqrt{n^2 - \frac{b^2}{\rho^2}}}. \quad (14)$$

To discuss the deflection angle and extract information of the MFE-like profile, the GBT was used instead of the null geodesics method. The GBT is calculated using the negative Gauss curvature of the optical metric.

2.1. Case 1

Let us start from the constant case for medium n_m as refractive index:

$$n_m = n_0, \quad (15)$$

where n_0 is a constant refractive index of the medium; here, we consider the GBT to obtain the deflection angle in a medium in weak field limits.

Let us write the optical Schwarzschild spacetime in an equatorial plane [45]:

$$d\sigma^2 = \frac{n_m^2}{f(\rho)}[g(\rho)d\rho^2 + \rho^2 d\varphi^2]. \quad (16)$$

Then, we calculate the Gaussian optical curvature:

$$K = -2 \frac{M}{n_0^2 \rho^3} + 3 \frac{M^2}{n_0^2 \rho^4} + O(M^3), \quad (17)$$

which is negative everywhere that gives a universal property of black-hole metrics [23].

It reduces to this form at a linear order of M :

$$K \approx -2 \frac{M}{n_0^2 \rho^3}. \quad (18)$$

This result is used to evaluate the deflection angle using a nonsingular domain outside the light ray (D_ρ , with boundary $\partial D_\rho = \gamma \cup C_\rho$) [22]:

$$\iint_{D_\rho} K dS + \oint_{\partial D_\rho} \kappa dt + \sum_i \theta_i = 2\pi\chi(D_\rho), \quad (19)$$

where κ stands for the geodesic curvature, and K is the Gaussian optical curvature, with exterior angles $\theta_i = (\theta_O, \theta_S)$ and Euler characteristic number $\chi(D_\rho) = 1$. At weak limits, ($\rho \rightarrow \infty$), $\theta_O + \theta_S \rightarrow \pi$. Then, the GBT reduces to

$$\iint_{D_\rho} K dS + \oint_{C_\rho} \kappa dt \stackrel{\rho \rightarrow \infty}{=} \iint_{D_\infty} K dS + \int_0^{\pi+\hat{\alpha}} d\varphi = \pi. \quad (20)$$

For geodesics γ , geodesic curvature vanishes $\kappa(\gamma) = 0$, and we have

$$\kappa(C_\rho) = |\nabla_{\dot{C}_\rho} \dot{C}_\rho|, \quad (21)$$

with $C_\rho = \rho = \text{constant}$. The GBT becomes

$$\lim_{\rho \rightarrow \infty} \int_0^{\pi+\hat{\alpha}} \left[\kappa \frac{d\sigma}{d\varphi} \right] \Big|_{C_\rho} d\varphi = \pi - \lim_{\rho \rightarrow \infty} \iint_{D_\rho} K dS, \quad (22)$$

and one can calculate

$$\frac{d\sigma}{d\varphi} \Big|_{C_\rho} = n_m \left(\frac{\rho^3}{\rho - 2M} \right)^{1/2}, \quad (23)$$

where, for very large radial distance,

$$\kappa(C_\rho) dt = d\varphi. \quad (24)$$

Therefore, as expected, for this number density profile and physical metric (which imply that the optical metric is asymptotically Euclidean), we corroborate that

$$\lim_{\rho \rightarrow \infty} \kappa \frac{d\sigma}{d\varphi} \Big|_{C_\rho} = 1. \quad (25)$$

At a linear order in M , it follows to use Equation (22) in limit $\rho \rightarrow \infty$, and taking geodesic curve γ , approximated by its flat Euclidean version parametrized as $\rho = b/\sin \varphi$, with b representing the impact parameter in the physical spacetime that

$$\hat{\alpha} = - \lim_{\rho \rightarrow \infty} \int_0^\pi \int_{\frac{b}{\sin \varphi}}^\rho K dS. \quad (26)$$

After nontrivial calculation, we calculate that the deflection angle of the Schwarzschild black hole in medium for the leading order terms is

$$\hat{\alpha} = 4 \frac{M}{n_0 b}, \quad (27)$$

which agrees with the well-known results in the limit at which its presence is negligible ($n_0 = 1$); this expression reduces to known vacuum formula $\hat{\alpha} = 4 \frac{M}{b}$, so that GBT exhibits a partially topological effect. This method can be used in any asymptotically flat Riemannian optical metrics.

2.2. Case 2

Now, we apply the different model of the MFE-like medium [10]

$$n = \frac{z_0}{1 + z^2}, \quad (28)$$

where z_0 and z are a constant.

The Gaussian curvature of the optical metric approximating in leading orders is negative everywhere and found as:

$$K = -2 \frac{(z^2 + 1)^2 M}{z_0^2 \rho^3} + O(M^3), \quad (29)$$

Then, using the same method, we calculate the deflection angle as follows:

$$\hat{\alpha} \simeq 4 \frac{Mz^2}{z_0 b} + 4 \frac{M}{z_0 b}. \quad (30)$$

At $z = 0$ and $z_0 = 1$, it reduces to the exact Schwarzschild case.

2.3. Case 3

The refractive index for the dark-matter medium [50]

$$n(\omega) = 1 + \beta A_0 + A_2 \omega^2 \quad (31)$$

where $\beta = \frac{\rho_0}{4m^2\omega^2}$ and ρ_0 are the mass density of the scattered dark-matter particles, and $A_0 = -2\varepsilon^2 e^2$ and $A_{2j} \geq 0$.

The terms in $\mathcal{O}(\omega^2)$ and higher are related to the polarizability of the dark-matter candidate. Note that the order of ω^{-2} is due to the charged dark-matter candidate and ω^2 for a neutral dark-matter candidate. Moreover, there may be a linear term in ω when parity and charge-parity asymmetries are present.

The Gaussian curvature is obtained as:

$$K \approx -2 \frac{M}{(A_2 \omega^2 + \beta A_0 + 1)^2 \rho^3} + O(M^3) \quad (32)$$

The deflection angle is found as follows:

$$\hat{\alpha} = 4 \frac{M}{(A_2 \omega^2 + 1) b} - 4 \frac{MA_0}{(A_2 \omega^2 + 1)^2 b} \beta + O(\beta^2) \quad (33)$$

The effect of dark matter can be seen by comparison with the above deflection angle by the Schwarzschild black hole. Hence, dark matter gives a small deflection angle compared to the standard case.

3. Effect of Medium on Deflection Angle of Schwarzschild-Like Wormhole Using Gauss–Bonnet Theorem

In this section, we consider the static Schwarzschild-like wormhole solution [58] with metric

$$ds^2 = -(1 - 2M/r + \lambda^2)dt^2 + \frac{dr^2}{1 - 2M/r} + r^2 d\Omega_{(2)}^2, \quad (34)$$

which reduces to the black-hole metric in Equation (4) at $\lambda = 0$. Using the transformation of $t \rightarrow t/\sqrt{1 + \lambda^2}$ and $M \rightarrow M(1 + \lambda^2)$, the metric functions of the Schwarzschild-like wormhole spacetime become:

$$f(r) = 1 - \frac{2M}{r}, \quad g(r)^{-1} = 1 - \frac{2M(1 + \lambda^2)}{r}. \quad (35)$$

3.1. Case 1

We first use the constant profile as refractive $n_m = n_0$ to calculate the deflection angle in the medium in weak field limits. Using the same procedure, we obtain the optical metric, and calculate the Gaussian optical curvature for the Schwarzschild-like wormhole at a linear order of M as follows:

$$K \approx -\frac{(\lambda^2 + 2) M}{\rho^3 n_0^2} + O(M^3), \quad (36)$$

and after similar calculations, the corresponding deflection angle in the leading order terms is

$$\hat{\alpha} = 2 \frac{M\lambda^2}{n_0 b} + 4 \frac{M}{n_0 b}, \quad (37)$$

which agrees with the well-known results in the limit in which the medium is negligible ($n_0 = 1$) [42].

3.2. Case 2

To see the effect of the MFE-like medium, we use [10]

$$n = \frac{z_0}{1 + z^2}, \quad (38)$$

where z_0 and z are a constant. The Gaussian curvature of the optical metric approximating in leading orders is negative everywhere and found as:

$$K \approx -\frac{(z^2 + 1)^2 (\lambda^2 + 2) M}{\rho^3 z_0^2} \quad (39)$$

Using the GBT, the deflection angle is calculated as follows:

$$\hat{\alpha} \simeq 2 \frac{M\lambda^2 z^2}{z_0 b} + 2 \frac{M\lambda^2}{z_0 b} + 4 \frac{Mz^2}{z_0 b} + 4 \frac{M}{z_0 b}. \quad (40)$$

At $z = 0$ and $z_0 = 1$, it reduces to the previous result [42].

3.3. Case 3

Finally, we use the refractive index for dark matter given in Equation (31) to calculate the deflection angle of a wormhole in a medium. The Gaussian curvature is obtained as:

$$K \approx -\frac{(\lambda^2 + 2) M}{\rho^3 (A_2 \omega^2 + A_0 \beta + 1)^2} \quad (41)$$

The deflection angle is found as follows:

$$\hat{\alpha} = 2 \frac{M\lambda^2}{(A_2 \omega^2 + A_0 \beta + 1) b} + 4 \frac{M}{(A_2 \omega^2 + A_0 \beta + 1) b} \quad (42)$$

We find that the deflected photon through dark matter around the Schwarzschild-like wormhole has a large deflection angle compared to the standard case.

4. Conclusions

We calculated the deflection angle of black holes and wormholes in a dark-matter medium using the GBT. This was achieved by constructing optical metrics. In summary, we investigated that GBT is a partially topological effect. We demonstrated this by using three different cases. In the first case, we used the constant profile as a refractive index. Then, by constructing the optical geometry and using the GBT, we obtained the deflection angle in the weak field limit. The deflection angle of

the Schwarzschild black hole was correctly calculated in a medium that has a constant n_0 refractive index. In the second case, we used the MFE-like model (but uniform in large distances), repeated the calculation, and showed that it produces a similar effect.

In Section 2, we repeated our method on the Schwarzschild-like wormhole to see the effect of the dark-matter medium when light is propagated through it. Note that we supposed that the refractive index is spatially nonuniform as long as it is uniform at large distances. In the first case, we again used the constant refractive index, we considered the MFE-like profile, and, finally, the medium for the dark matter was taken to find the deflection angle in the weak field limit. We concluded that the deflection angle by a black hole decreases in a medium of dark matter, as seen in Equation (33). On the other hand, deflection angle by a wormhole increases, as seen in Equation (42).

These results suggest that weak deflection within a dark-matter medium or MFE-like model (perfect imaging), can be calculated using the Gibbons and Werner method, which gives us hints to understanding the nature of dark matter.

Funding: This work was supported by Comisión Nacional de Ciencias y Tecnología of Chile through FONDECYT Grant No. 3170035 (A.Ö.)

Acknowledgments: A.Ö. is grateful to the Institute for Advanced Study, Princeton for their hospitality.

Conflicts of Interest: The author declares no conflict of interest. The funders had no role in the design of the study; in the collection, analyses, or interpretation of data; in the writing of the manuscript; or in the decision to publish the results.

References

1. Abbott, B.P.; Abbott, R.; Abbott, T.D.; Abernathy, M.R.; Acernese, F.; Ackley, K.; Adams, C.; Adams, T.; Addesso, P.; Adhikari, R.X.; et al. Observation of Gravitational Waves from a Binary Black Hole Merger. *Phys. Rev. Lett.* **2016**, *116*, 061102. [CrossRef]
2. Nutku, Y.; Halil, M. Colliding Impulsive Gravitational Waves. *Phys. Rev. Lett.* **1977**, *39*, 1379–1382. [CrossRef]
3. Alberdi, A.; Gómez Fernández, J.L.; Event Horizon Telescope Collaboration. First M87 Event Horizon Telescope Results. I. The Shadow of the Supermassive Black Hole. Available online: <http://adsabs.harvard.edu/abs/2019ApJ...875L...1E> (accessed on 13 May 2019).
4. Giddings, S.B.; Psaltis, D. Event Horizon Telescope Observations as Probes for Quantum Structure of Astrophysical Black Holes. *Phys. Rev. D* **2018**, *97*, 084035. [CrossRef]
5. Barrau, A. Astrophysical and cosmological signatures of Loop Quantum Gravity. *Scholarpedia* **2017**, *12*, 33321. [CrossRef]
6. Niven, W.D. *The Scientific Papers of James Clerk Maxwell*; Maxwell's Original Piece in the Cambridge and Dublin Mathematical Journal for February 1854; Cambridge University Press: Cambridge, UK, 1890; Volume 1, pp. 76–79.
7. Pendry, J.B. Negative Refraction Makes a Perfect Lens. *Phys. Rev. Lett.* **2000**, *85*, 3966–3969. [CrossRef]
8. Luneburg, R.K. *Mathematical Theory of Optics*; Brown University: Providence, RI, USA, 1944; pp. 189–213.
9. Leonhardt, U. Perfect imaging without negative refraction. *New J. Phys.* **2009**, *11*, 093040. [CrossRef]
10. Leonhardt, U.; Sahebdivan, S. Theory of Maxwell's fish eye with mutually interacting sources and drains. *Phys. Rev. A* **2015**, *92*, 053848. [CrossRef]
11. Leonhardt, U. Optical conformal mapping. *Science* **2006**, *312*, 1777–1780. [CrossRef]
12. Minano, J.C. Perfect imaging in a homogeneous three-dimensional region. *Opt. Express* **2006**, *14*, 9627–9635. [CrossRef]
13. Tyc, T.; Danner, A. Resolution of Maxwell's fisheye with an optimal active drain. *New J. Phys.* **2014**, *16*, 063001. [CrossRef]
14. Liu, Y.; Chen, H. Infinite Maxwell fisheye inside a finite circle. *J. Opt.* **2015**, *17*, 125102. [CrossRef]
15. Guenneau, S.; Diatta, A.; McPhedran, R.C. Focusing: coming to the point in metamaterials. *J. Mod. Opt.* **2010**, *57*, 511–527. [CrossRef]
16. Perlick, V. Gravitational Lensing from a Spacetime Perspective. *Living Rev. Relat.* **2004**, *7*, 9. [CrossRef]
17. Bozza, V. Gravitational Lensing by Black Holes. *Gen. Relat. Grav.* **2010**, *42*, 2269–2300. [CrossRef]

18. Stefanov, I.Z.; Yazadjiev, S.S.; Gylchev, G.G. Connection between Black-Hole Quasinormal Modes and Lensing in the Strong Deflection Limit. *Phys. Rev. Lett.* **2010**, *104*, 251103. [[CrossRef](#)]
19. Epps, S.D.; Hudson, M.J. The Weak Lensing Masses of Filaments between Luminous Red Galaxies. *Mon. Not. R. Astron. Soc.* **2017**, *468*, 2605–2613. [[CrossRef](#)]
20. Bartelmann, M.; Schneider, P. Weak gravitational lensing. *Phys. Rept.* **2001**, *340*, 291–472. [[CrossRef](#)]
21. Ade, P.A.; Aghanim, N.; Arnaud, M.; Ashdown, M.; Aumont, J.; Baccigalupi, C.; Banday, A.J.; Barreiro, R.B.; Bartlett, J.G.; Bartolo, N.; et al. Planck 2015 results. XIII. Cosmological parameters. *Astron. Astrophys.* **2016**, *594*, A13.
22. Gibbons, G.W.; Werner, M.C. Applications of the Gauss-Bonnet theorem to gravitational lensing. *Class. Quant. Grav.* **2008**, *25*, 235009. [[CrossRef](#)]
23. Gibbons, G.W.; Warnick, C.M. Universal properties of the near-horizon optical geometry. *Phys. Rev. D* **2009**, *79*, 064031. [[CrossRef](#)]
24. Werner, M.C. Gravitational lensing in the Kerr-Randers optical geometry. *Gen. Relat. Grav.* **2012**, *44*, 3047. [[CrossRef](#)]
25. Ishihara, A.; Suzuki, Y.; Ono, T.; Kitamura, T.; Asada, H. Gravitational bending angle of light for finite distance and the Gauss-Bonnet theorem. *Phys. Rev. D* **2016**, *94*, 084015. [[CrossRef](#)]
26. Sakalli, I.; Ovgun, A. Hawking Radiation and Deflection of Light from Rindler Modified Schwarzschild Black Hole. *Europhys. Lett.* **2017**, *118*, 60006. [[CrossRef](#)]
27. Jusufi, K.; Werner, M.C.; Banerjee, A.; Övgün, A. Light Deflection by a Rotating Global Monopole Spacetime. *Phys. Rev. D* **2017**, *95*, 104012. [[CrossRef](#)]
28. Ono, T.; Ishihara, A.; Asada, H. Gravitomagnetic bending angle of light with finite-distance corrections in stationary axisymmetric spacetimes. *Phys. Rev. D* **2017**, *96*, 104037. [[CrossRef](#)]
29. Jusufi, K.; Sakalli, I.; Övgün, A. Effect of Lorentz Symmetry Breaking on the Deflection of Light in a Cosmic String Spacetime. *Phys. Rev. D* **2017**, *96*, 024040.
30. Ishihara, A.; Suzuki, Y.; Ono, T.; Asada, H. Finitedistance corrections to the gravitational bending angle of light in the strong deflection limit. *Phys. Rev. D* **2017**, *95*, 044017. [[CrossRef](#)]
31. Jusufi, K.; Övgün, A.; Banerjee, A. Light deflection by charged wormholes in Einstein-Maxwell-dilaton theory. *Phys. Rev. D* **2017**, *96*, 084036. [[CrossRef](#)]
32. Arakida, H. Light deflection and Gauss-Bonnet theorem: Definition of total deflection angle and its applications. *Gen. Relat. Grav.* **2018**, *50*, 48. [[CrossRef](#)]
33. Jusufi, K.; Övgün, A. Gravitational Lensing by Rotating Wormholes. *Phys. Rev. D* **2018**, *97*, 024042. [[CrossRef](#)]
34. Övgün, A.; Sakalli, I.; Saavedra, J. Shadow cast and Deflection angle of Kerr-Newman-Kasuya spacetime. *J. Cosmol. Astropart. Phys.* **2018**, *1810*, 41. [[CrossRef](#)]
35. Övgün, A.; Sakalli, I.; Saavedra, J. Weak gravitational lensing by Kerr-MOG Black Hole and Gauss-Bonnet theorem. *arXiv* **2018**, arXiv:1806.06453.
36. Övgün, A.; Gylchev, G.; Jusufi, K. Weak Gravitational lensing by phantom black holes and phantom wormholes using the Gauss-Bonnet theorem. *Ann. Phys.* **2019**, *406*, 152–172. [[CrossRef](#)]
37. Jusufi, K.; Övgün, A.; Saavedra, J.; Gonzalez, P.A.; Vasquez, Y. Deflection of light by rotating regular black holes using the Gauss-Bonnet theorem. *Phys. Rev. D* **2018**, *87*, 124024. [[CrossRef](#)]
38. Övgün, A.; Jusufi, K.; Sakalli, I. Exact traversable wormhole solution in bumblebee gravity. *Phys. Rev. D* **2019**, *99*, 024042. [[CrossRef](#)]
39. Övgün, A.; Jusufi, K.; Sakalli, I. Gravitational lensing under the effect of Weyl and bumblebee gravities: Applications of Gauss–Bonnet theorem. *Ann. Phys.* **2018**, *399*, 193–203. [[CrossRef](#)]
40. Jusufi, K.; Övgün, A. Effect of the cosmological constant on the deflection angle by a rotating cosmic string. *Phys. Rev. D* **2018**, *97*, 064030. [[CrossRef](#)]
41. Javed, W.; Babar, R.; Övgün, A. The effect of the Brane-Dicke coupling parameter on weak gravitational lensing by wormholes and naked singularities. *Phys. Rev. D* **2019**, *99*, 084012. [[CrossRef](#)]
42. Övgün, A. Light deflection by Damour-Solodukhin wormholes and Gauss-Bonnet theorem. *Phys. Rev. D* **2018**, *98*, 044033. [[CrossRef](#)]
43. Ono, T.; Ishihara, A.; Asada, H. Deflection angle of light for an observer and source at finite distance from a rotating wormhole. *Phys. Rev. D* **2018**, *98*, 044047. [[CrossRef](#)]
44. Ono, T.; Ishihara, A.; Asada, H. Deflection angle of light for an observer and source at finite distance from a rotating global monopole. *arXiv* **2018**, arXiv:1811.01739.

45. Crisnejo, G.; Gallo, E. Weak lensing in a plasma medium and gravitational deflection of massive particles using the Gauss-Bonnet theorem. A unified treatment. *Phys. Rev. D* **2018**, *97*, 124016. [[CrossRef](#)]
46. Crisnejo, G.; Gallo, E.; Rogers, A. Finite distance corrections to the light deflection in a gravitational field with a plasma medium. *arXiv* **2018**, arXiv:1807.00724.
47. Asada, H. Gravitational lensing by exotic objects. *Mod. Phys. Lett. A* **2017**, *32*, 1730031. [[CrossRef](#)]
48. Hinshaw, G.; Larson, D.; Komatsu, E.; Spergel, D.N.; Bennett, C.; Dunkley, J.; Nolte, M.R.; Halpern, M.; Hill, R.S.; Odegard, N.; et al. Nine-Year Wilkinson Microwave Anisotropy Probe (WMAP) Observations: Cosmological Parameter Results. *Astrophys. J. Suppl.* **2013**, *208*, 19. [[CrossRef](#)]
49. Feng, J.L. Dark Matter Candidates from Particle Physics and Methods of Detection. *Ann. Rev. Astron. Astrophys.* **2010**, *48*, 495. [[CrossRef](#)]
50. Latimer, D.C. Dispersive Light Propagation at Cosmological Distances: Matter Effects. *Phys. Rev. D* **2013**, *88*, 063517. [[CrossRef](#)]
51. Latimer, D.C. Anapole dark matter annihilation into photons. *Phys. Rev. D* **2017**, *95*, 095023. [[CrossRef](#)]
52. Latimer, D.C. Two-photon interactions with Majorana fermions. *Phys. Rev. D* **2016**, *94*, 093010. [[CrossRef](#)]
53. Kvam, A.K.; Latimer, D.C. Optical dispersion of composite particles consisting of millicharged constituents. *J. Phys. G* **2016**, *43*, 085002. [[CrossRef](#)]
54. Whitcomb, K.M.; Latimer, D.C. Scattering from a quantum anapole at low energies. *Am. J. Phys.* **2017**, *85*, 932. [[CrossRef](#)]
55. Tsupko, O.Y.; Bisnovatyi-Kogan, G.S. Gravitational lensing in plasma: Relativistic images at homogeneous plasma. *Phys. Rev. D* **2013**, *87*, 124009. [[CrossRef](#)]
56. Bisnovatyi-Kogan, G.S.; Tsupko, O.Y. Gravitational lensing in a non-uniform plasma. *Mon. Not. R. Astron. Soc.* **2010**, *404*, 1790–1800. [[CrossRef](#)]
57. Bisnovatyi-Kogan, G.S.; Tsupko, O.Y. Gravitational Lensing in Plasmic Medium. *Plasma Phys. Rep.* **2015**, *41*, 562–581. [[CrossRef](#)]
58. Damour, T.; Solodukhin, S.N. Wormholes as black hole foils. *Phys. Rev. D* **2007**, *76*, 024016. [[CrossRef](#)]



© 2019 by the authors. Licensee MDPI, Basel, Switzerland. This article is an open access article distributed under the terms and conditions of the Creative Commons Attribution (CC BY) license (<http://creativecommons.org/licenses/by/4.0/>).